

# Hydrothermal Synthesis, Optostructural, Compositional and Electrochemical Photovoltaic Properties of Nanocrystalline TiO<sub>2</sub>-ZnO Composite Thin Films

D. B. Shinde<sup>1</sup>, P. N. Bhosale<sup>2</sup>, R. K. Mane<sup>3</sup>

<sup>1</sup>S.P.K. Mahavidyalaya, Sawantwadi-416510, Dist. Sindhudurg, India

<sup>2</sup>Materials Research Laboratory, Department of Chemistry, Shivaji University, Kolhapur-416004, India

<sup>3</sup>Smt. K.R.P.Kanya Mahavidyalaya, Islampur-415409, Dist.-Sangli, India

**Abstract:** *In the present investigation, we report facile synthesis of TiO<sub>2</sub>-ZnO nanocomposite thin films. High density TiO<sub>2</sub> nanorods were hydrothermally deposited on transparent conducting oxide substrate followed by deposition of ZnO nanorods by simple chemical reflux method at low temperature. The structural, optical, morphological, compositional and electrochemical properties are investigated by detailed XRD, UV-Vis-NIR spectrophotometer, photoluminescence spectrophotometer, SEM, TEM, EDAX, XPS and photoelectrochemical studies. Optical spectra showed strong light absorption in UV region. The XRD spectra and TEM examination demonstrated that, the TiO<sub>2</sub>-ZnO nanocomposite consist pure rutile phase tetragonal TiO<sub>2</sub> nanorods and wurtzite phase hexagonal ZnO nanorods. The SEM images confirm uniform, compact and well aligned nanorods were grown on the overall substrate surface. EDAX and XPS Spectra confirm the formation of pure TiO<sub>2</sub>-ZnO nanocomposite. The TiO<sub>2</sub>-ZnO composite materials showed photo efficiency  $\eta = 3.8\%$ .*

**Keywords:** Single crystalline, Nanocomposite architecture, Photoelectrochemical cell property, Photoconversion efficiency

## 1. Introduction

There has been increasing interest during the last few decades to find out an alternative cost effective renewable energy sources to fulfill the future energy needs of mankind. In this respect synthesis of tailored morphological mixed transitional metal oxide (TMO) semiconducting thin films because of their widespread applications in optoelectronic fields of science and technology leading to drastic cut in the production cost of semiconducting devices[1-4].

Recently, considerable interest has focused on synthesis of nanocomposite films and powders such as TiO<sub>2</sub>-ZnO, TiO<sub>2</sub>-SiO<sub>2</sub>, TiO<sub>2</sub>-WO<sub>3</sub>, and TiO<sub>2</sub>-CdSe which have been considered as effective semiconductors [5-8]. Many attempts have been made to synthesize coupled bicomponent ZnO-TiO<sub>2</sub> nanocomposite by a physical or chemical process with two aims, (i) extending the light adsorption spectrum and improving the conversion efficiency and (ii) suppressing the recombination of photogenerated electron/hole pairs. This nanocomposite may increase the PEC conversion efficiency by increasing the charge separation and extending the photoresponding range [9].

In this context, there has been considerable effort made toward the investigation of TiO<sub>2</sub>-ZnO nanocomposite, however, to the best of our knowledge, little attention has been paid to the coupling of ZnO and TiO<sub>2</sub> nanorod structures. Therefore considering the above fact and literature survey, in the present attempt we synthesize and studied TiO<sub>2</sub>-ZnO nanocomposite thin films.

## 2. Method and Materials

Fluorine doped tin oxide (FTO) coated glass substrates with a sheet resistance of 25 $\Omega$ cm<sup>-2</sup> used as a conducting substrate support for deposition. All chemical reagents used were analytical reagent (AR) grade. Zinc acetate dihydrate (Zn(CH<sub>3</sub>COO)<sub>2</sub>·2H<sub>2</sub>O), hexamethylenetetraamine (HMTA) ((CH<sub>2</sub>)<sub>6</sub>N<sub>4</sub>) used as the Zn precursor. Titanium tetraisopropoxide (TTIP)(99.98% Spectrochem, India), Concentrated hydrochloric acid (35.4% Thomas Baker) used as the Ti precursor. The aqueous solution was prepared using double distilled water. The substrates were washed with detergent and then cleaned with double distilled water and acetone separately in an ultrasonic bath.

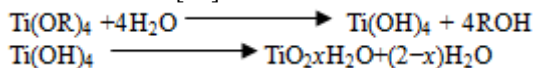
## 3. Thin Film Synthesis

In a typical TiO<sub>2</sub> thin film synthesis 0.5 ml titanium tetra isopropoxide (TTIP) was added in aqueous solution containing 1:1 HCl and stirred vigorously for to obtained clear and transparent solution. The resultant solution was added into teflon lined stainless steel autoclave. The conducting FTO glass substrate is immersed into autoclave solution and autoclave was sealed and placed in an oven at 160°C for 3 hr/ 5 hr followed by natural cooling to room temperature. The substrate was removed from autoclave, cooled at room temperature and rinsed thoroughly using double distilled water. 50 ml of zinc acetate dihydrate and 50 ml of HMTA solutions were prepared in double distilled water. These two solutions were mixed and stirred for 10 minutes. The TiO<sub>2</sub> deposited FTO substrate were dipped in

the solution and refluxed at  $77 \pm 2$  °C for 3 hr/ 5 hr to deposit pure ZnO thin film. Finally, the substrates were washed with double distilled water, dried at room temperature and used for further characterization without post annealing treatment.

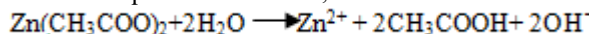
#### 4. Possible Growth Mechanism

The FTO substrates were used for the growth of 3D nanostructures  $\text{TiO}_2$ -ZnO, because due to the lattice mismatch bare glass substrates have been unsuccessful for this purpose [10]. The addition of aqueous HCl causes the hydrolysis of the inorganic moieties. Under acidic conditions, the transformation of  $\text{Ti}^{2+}$  from  $\text{Ti}^{4+}$  avoided and stabilizes the oxidation state of  $\text{Ti}^{4+}$  [11].

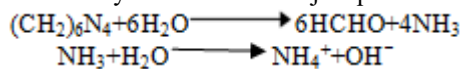


The  $\text{Cl}^-$  ions adsorbed at the (110) facets having higher density of Ti atoms. Hence there would be an interaction between Ti atoms and n-donor base  $\text{Cl}^-$ . This facilitate the anisotropic growth along (110) facets and decreases the growth rate along (001) facets which leads to the formation of rutile phase  $\text{TiO}_2$  nanorods instead of particles [12].

To deposit  $\text{TiO}_2$ -ZnO nanocomposite thin film aqueous zinc acetate is used. Initially, zinc acetate dissociates as  $\text{Zn}^{2+}$  and acetic acid in aqueous medium as,



The HMTA reacts with water and form formaldehyde and ammonia. Ammonia formed in this reaction helps for the formation of zinc hydroxide and to adjust pH of the solution,



The hydroxide ions formed in above reaction react with  $\text{Zn}^{2+}$  ions to form zinc hydroxide,



During the reflux at  $77 \pm 2$  °C for 5 hours zinc hydroxide deposited on  $\text{TiO}_2$  deposited FTO glass substrate and loses water molecules and form ZnO as,



The hexagonal wurtzite ZnO nanorods are aggregated and connect with one root leading to formation of 3D nanorod flowers on the top surface of  $\text{TiO}_2$  nanorods [13].

#### 5. Optical Absorbance Study

UV-Vis-NIR absorption spectra of the deposited  $\text{TiO}_2$ -ZnO film were recorded in the range of 300-800 nm is shown in Fig.1(a). The absorption spectra reveals the strong absorption at 370 nm indicated a charge transfer process from the valence band to conduction band in the UV region. Generally, the wide band gap semiconductor materials such as,  $\text{TiO}_2$  and ZnO shows the maximum light absorption in UV region of the solar spectrum. Using the absorption edge value, band gap was calculated according to the Tauc relation, i.e.  $(\alpha h\nu)^2$  vs.  $h\nu$ . The nature of transition in film is confirmed by equation (1).

$$\alpha h\nu = \alpha (h\nu - E_g)^n \quad (1)$$

Where, „A“ is an energy dependant constant, „ $E_g$ “ is the band gap energy and „ $h\nu$ “ is the photon energy. The absorption

coefficient is near the fundamental absorption edge, which allows absorption of light even for a small thickness [14]. The plot of  $(\alpha h\nu)^2$  vs.  $h\nu$  gives straight line at higher energies indicating direct type of transition.

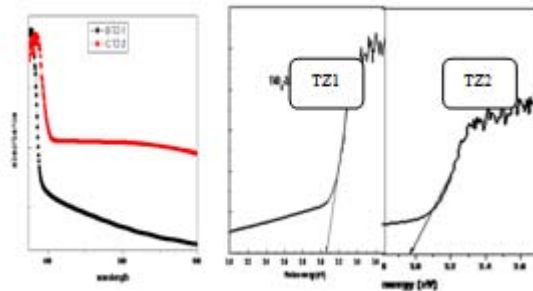


Figure 1: (a) UV-Vis-NIR absorption spectra, (b and c) shows plot of  $(\alpha h\nu)^2$  vs.  $h\nu$  of  $\text{TiO}_2$ -ZnO thin films.

The intercept of the extrapolation to zero absorption with the photon energy axis is taken as the value of band gap ( $E_g$ ) shown in Fig.1(b and c). The band gap of deposited  $\text{TiO}_2$ -ZnO thin films were found 2.95 and 3.05 eV respectively and the thickness of thin films were 1 micron and 1.3 micron resp.

#### 5.1 Structural Study

The crystallite size and crystal structure of  $\text{TiO}_2$ -ZnO thin films were confirmed from the XRD analysis. Fig.2 shows XRD pattern of all the samples. XRD patterns exhibited strong diffraction peaks at  $27.55^\circ$ ,  $36.79^\circ$  and  $55.40^\circ$  indicating formation of pure hexagonal wurtzite phase ZnO and tetragonal rutile phase of  $\text{TiO}_2$  material. The intense peak at  $27.55^\circ$  is the representative peak for (110) plane of rutile  $\text{TiO}_2$ .

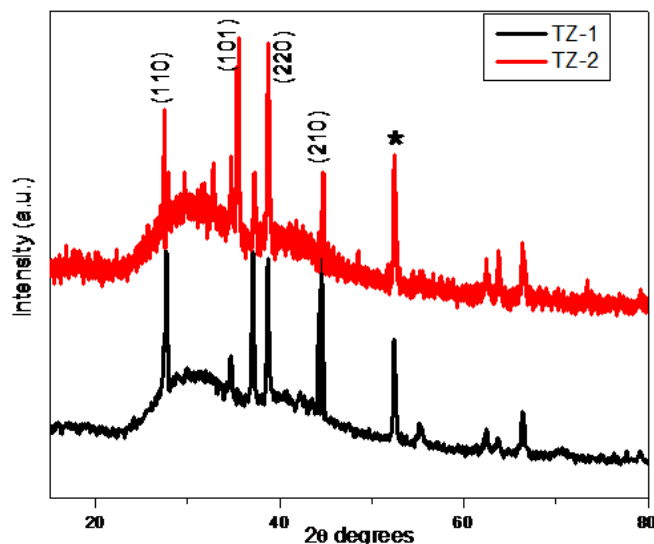


Figure 2: XRD pattern of  $\text{TiO}_2$ -ZnO thin film samples

All other peaks observed at  $36.79^\circ$ ,  $39.12^\circ$ ,  $41.42^\circ$ ,  $44.29^\circ$ ,  $55.40^\circ$ ,  $62.72^\circ$  and  $64.29^\circ$  confirms  $\text{TiO}_2$ -ZnO nanocomposite consist pure rutile phase tetragonal  $\text{TiO}_2$  nanorods and wurtzite phase hexagonal ZnO nanorods. All peaks are in good agreement with the standard JCPDS data (Card no. 80-0078 and Card No. 00 001-0562) [15]. The other peaks shown by asterisks are due to the FTO substrate marked by \*. No other impurity peak in XRD pattern indicating no traces of secondary phases were observed. The presence of broad

XRD peaks is an indication of small crystallite size in the range of nanoscale, affirming the nanocrystalline nature of the samples. Average crystallite size of TiO<sub>2</sub>-ZnO samples were calculated by using Scherrer's formula shown in equation (2).

$$D = \frac{0.94 \lambda}{\beta \cos \theta} \quad (2)$$

Where „D“ is the crystallite size, „θ“ is peak position of X-ray used, „β“ is full width at half maxima (FWHM) and „λ“ is wavelength of X-ray used (0.154 nm). The calculated crystallite size of TiO<sub>2</sub>-ZnO for (110) planes are found to be 16.47 nm.

### 5.2 Morphological Study

Fig.3(a, b) shows SEM images of the composite TiO<sub>2</sub>-ZnO nanorods. It shows smooth, completely grown and regularly arranged nanorods at the bottom layer with irregularly arranged nanorod flowers on their top surface. There is formation of 3D nanorod flowers with diameter 2 μm aggregated on the surface of the substrate, which exhibit step by step growth process. This kind of nanorods and flowers on the top surface of nanorods are densely and uniformly covered the whole surface of the substrate.

To investigate the detailed structure and crystallinity of TiO<sub>2</sub>-ZnO nanocomposite, TEM analysis is performed. Fig.4(a) shows the TEM image focused on a single nanorod. A nanorod is having 100 to 150 nm diameter and a tetragonal architecture with a smooth surface. The sharp SAED pattern shown in Fig.4(b) the bright dotted pattern indicates that the nanorod is single crystalline.

The Fig.4(c) shows the HRTEM pattern of TiO<sub>2</sub>-ZnO sample. It indicates that the nanorods are completely crystalline along the entire lengths with the lattice spacing

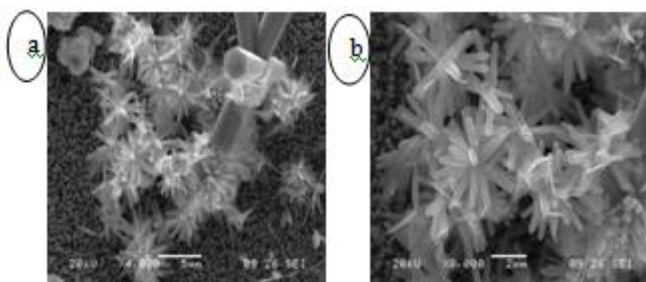


**Figure 3 (a, b):** SEM images of TiO<sub>2</sub>-ZnO thin film samples

0.344 nm, corresponding to the d-spacing of the (110) plane of rutile TiO<sub>2</sub> and 0.24nm corresponds to (002) plane of wurtzite ZnO. The predominant growth directions are in good agreement with the XRD pattern [16-17].

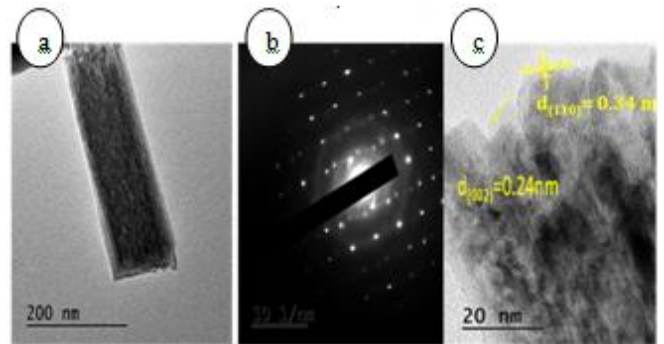


**Figure 4:** (a) shows TEM image, (b) SAED pattern and (c) HRTEM image of TiO<sub>2</sub>-ZnO sample.

### 5.3 Compositional Analysis

An elemental composition of TiO<sub>2</sub>-ZnO thin films was analyzed by EDS. Fig.5 shows an EDS pattern obtained for TiO<sub>2</sub>-ZnO sample. There is no trace of any other impurities could be seen within the detection limit of the EDS. The corresponding EDS results confirm the formation of ZnO, TiO<sub>2</sub> and TiO<sub>2</sub>-ZnO thin films.

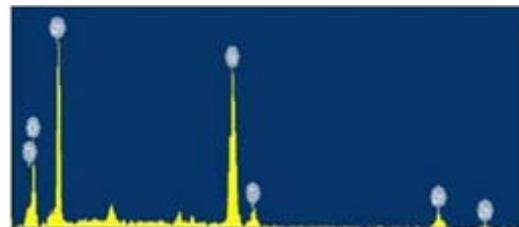


**Figure 5:** Shows Energy Dispersive X-ray (EDX) spectrum of TiO<sub>2</sub>-ZnO thin films.

The XPS analysis of ZnO, TiO<sub>2</sub> and TiO<sub>2</sub>-ZnO thin films were performed to identify the composition and valence state of elements. The survey spectrum of TiO<sub>2</sub>-ZnO sample is presented in Fig.6. It shows presence of Zn, Ti, O and a small amount of adventitious carbon. The carbon peak is attributed to the residual carbon from XPS instrument itself. The peak at binding energy 284.87 eV corresponds to amorphous carbon. The peaks at 1021.25 eV and 1044.36 eV assigned to the electronic states of Zn2P<sub>3/2</sub> and Zn2P<sub>1/2</sub>, respectively. It indicates that Zn ions exist in +2 oxidation state. Figure consists of the distinct Ti /2p<sub>1/2</sub> and Ti /2p<sub>3/2</sub> signals that are located at 464.4 and 458.6 eV respectively. The spin orbital splitting between these peaks is 5.8 eV which is comparable with that of 5.74 eV reported values, indicates Ti<sup>4+</sup> oxidation state [18].

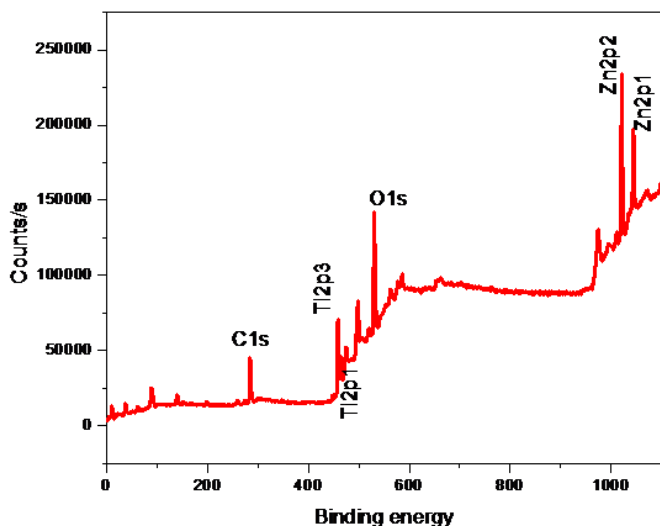


Figure 6: Experimental survey spectrum of TiO<sub>2</sub>-ZnO

#### 5.4. Photoelectrochemical Property

The metal oxide semiconductors can absorb large amount of light radiation to form photogenerated electron-hole pairs. The photogenerated electrons can transport directly through crystallites and compact layers to the conducting substrates with minimum loss. This photo generated electrons travel through the external load and completes the circuit by entering back through the counter electrode.

The J-V characteristic curve of TiO<sub>2</sub>-ZnO thin films under UV illumination in light and dark is shown in Fig. 7. The standard two electrode system was fabricated to study PEC property as,

Glass - FTO / TiO<sub>2</sub>-ZnO / 0.1 M Na<sub>2</sub>SO<sub>4</sub> / Graphite

The PEC parameters such as fill factor (FF) and PEC efficiency (η%) was calculated by Equation (3) and (4) given as,

$$FF = \frac{J_{max} V_{max}}{J_{sc} V_{oc}} \quad (3)$$

$$\eta \% = \frac{J_{sc} V_{oc}}{P_{in}} \times FF \times 100 \quad (4)$$

where, „*V*<sub>max</sub>’ is maximum voltage, „*J*<sub>max</sub>’ is maximum current density, „*J*<sub>sc</sub>’ is short circuit current density, „*V*<sub>oc</sub>’ is open circuit voltage and ‘*P*<sub>in</sub>’ is intensity of incident light.

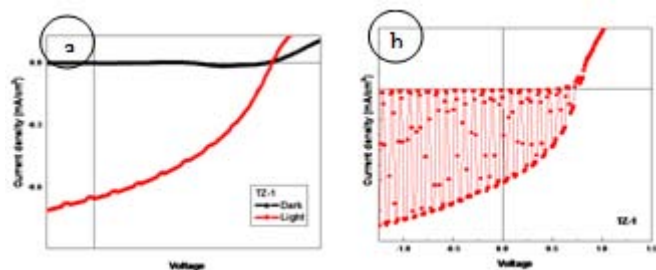


Figure 7 (a): J-V characteristic curve and (b) chopping curve of TiO<sub>2</sub>-ZnO nanostructure samples.

The photocurrent could not be detected unless nanostructured TiO<sub>2</sub>-ZnO photoanode illumines with UV light. When the nanostructure photoanode were illuminated under UV light, photovoltage were rises rapidly to a constant value causes shift in the fourth quadrant indicating the generation of

electricity, which are typical solar cell characteristics. These PEC parameters TiO<sub>2</sub>-ZnO sample is summarized in Table 1.

Table 1: The PEC output parameters of the sample TZ<sub>1</sub>.

<i>V</i> <sub>oc</sub> (mV)	<i>V</i> <sub>max</sub> (mV)	<i>J</i> <sub>sc</sub> (mA/cm <sup>2</sup> )	<i>J</i> <sub>max</sub> (mA/cm <sup>2</sup> )	FF	η %
747	414	0.654	0.463	0.39	3.8

The PEC measurement of nanocomposite TiO<sub>2</sub>-ZnO showed photoconversion efficiency η = 3.8%. An open circuit voltage-decay measurement was conducted to investigate recombination kinetics of nanostructure and is shown in Fig. 7(b). Adopting the technique reported by Zaban et al. open circuit voltage-decay measurements are performed. It showed that the response of these electrodes to UV illumination was very prompt [19].

#### 6. Conclusions

We have successfully demonstrated a simple and low cost synthesis method for deposition of composite TiO<sub>2</sub>-ZnO thin films having well aligned nanorod morphology. Optical measurements allowed to evaluate the energy gap values and to appreciate the occurrence of scattering effects due to the high surface area of the different structures coupled with their characteristic dimensions. SEM and TEM analysis evidenced the structural differences and the high degree of crystallinity of these materials. The PEC measurements showed that TiO<sub>2</sub>-ZnO composite thin films showed 3.8% conversion efficiency. The PEC performance has been attributed due to stronger light scattering effects, faster electron transportation and electrolyte diffusion in densely and uniformly covered TiO<sub>2</sub>-ZnO nanorod sample.

#### References

- [1] P. K. Santra and P. V. Kamat, “Mn-doped quantum dot sensitized solar cells: a strategy to boost efficiency”. J. Am. Chem. Soc., 134, (5) 2508-2511.
- [2] V. Manthina, J. P. C. Baena, G. Liu and A. G. Agrios, “ZnO–TiO<sub>2</sub> Nanocomposite films for high light harvesting efficiency and fast electron transport in dye sensitized solar cells”. J. Phys. Chem. C, 116, 23864.
- [3] R. Bel-Hadj-Tahar, A. B. Mohamed, “Sol-Gel processed Indium-Doped ZnO Thin Films and Their Electrical and Optical Properties, N.J. Glass and Ceramics, 4, 55-65.
- [4] R. A. Naphade, M. Tathavadekar, J. P. Jog, S. Agarkar and S. Ogale, (2014), Plasmonic light harvesting of dye sensitized solar cells by Au-nanoparticle loaded TiO<sub>2</sub> nanofiber. J. Mater. Chem. A, 2, 975-984.
- [5] E. Guo and L. Yin, “Nitrogen doped TiO<sub>2</sub>-Cu<sub>x</sub>O core-shell mesoporous spherical hybrids for high-performance dye-sensitized solar cells” J. Phys. Chem. Chem. Phys., 17, 563.
- [6] A. I. Ali, A. H. Ammar, A. A. Moez, “Influence of substrate temperature on structural, optical properties and dielectric results of nano- ZnO thin films, Superlat. and Microstr. 65, 285–298.
- [7] F. Li, J. He, W. L. Zhou and J. B. Wiley, “Synthesis of porous wires from directed assemblies of nanospheres”, J. Am. Chem. Soc., 125, 52, 16166.

- [8] Y. S. Kobayashi, H. Narita, T. Kanehira, K. Sonezaki, S. Kubota, Y. Terasaka, S. Iwasaki, "A review of electrode materials for electrochemical supercapacitors", *Photochem. Photobiol.*, 86, 964 - 971.
- [9] K. Hashimoto, H. Irie and A. Fujishima, "TiO<sub>2</sub> Photocatalysis: A historical overview and future prospects", *J. Appl. Phys.*, 44, 8269.
- [10] G. Wang, L. Zhang and J. Zhang, "A review of electrode materials for electrochemical supercapacitors, *Chem. Soc. Rev.*, 41, 797.
- [11] D. Liu, P. Xiao, Y. Zhang, B. B. Garcia, Q. Zhang, Q. Guo, R. Champion, and G. Cao, "TiO<sub>2</sub> Nanotube Arrays Annealed in N<sub>2</sub> for Efficient Lithium-Ion Intercalation" *J. Phys. Chem. C*, 112, 11175–11180.
- [12] Kaitsuka, Y. and Goto, H. "Preparation, Polyaniline ZnO Films by Electrochemical Polymerization, *Open Journal of Polymer Chemistry*, 6, 1.
- [13] R. Wang, K. Hashimoto, A. Fujishima, M. Chikuni, E. Kojima, A. Kitamura, M. Shimohigoshi, T. Watanabe, Light-Induced Amphi-philic Surfaces, *Nature*, 388, 1641, 431.
- [14] U. S. Mbamara, O. O. Akinwunmi, E. I. Obiajunwa, "Deposition and Characterisation of Nitrogen-Doped Zinc Oxide Thin Films by MOCVD Using Zinc Acetate-Ammonium Acetate Precursor", *J. Mod. Phys.*, 3, 652.
- [15] S. S. Mali, C. A. Betty, P. N. Bhosale, P. S. Patil, "Hydrothermal synthesis of rutile TiO<sub>2</sub> with hierarchical microspheres and their Characterization", *J. Cryst. Eng. Comm.*, 13, 6349-6351.
- [16] G. Poongodi, P. Anandan, R. M. Kumar, "Studies on visible light photocatalytic and antibacterial activities of nanostructured cobalt doped ZnO thin films prepared by sol-gel spin coating method, *Petrochimica Acta Part A: Mol. and Biomol. Spectro.*, 148, 237.
- [17] J. Li, W. Wan, H. Zhou, J. Li and, D. Xu, (2012) Nanotube based hierarchical titanate microspheres: an improved anode structure for Li-ion batteries, *Chem. Commun.*, 48, 389.
- [18] N. Chahmat, A. Haddad, A. Ain-Souya, R. Ganfoudi, "Effect of Sn Doping on the Properties of ZnO Thin Films Prepared by Spray Pyro". *J. Mod. Phys.*, 3, 1781.
- [19] C. W. Kim, U. Pal, S. Park, Y. H. Kim, J. Kim, "Crystallization Induced porosity control and photocatalytic activity of ordered mesoporous TiO<sub>2</sub>" *RSC Adv.*, 2, 11969.